Catal Lett (2009) 128:493–501
DOI 10.1007/s10562-008-9782-0

Direct Synthesis of Methyl Propionate from *n*-Propyl Alcohol and Methanol Using Gold Catalysts

Guangliang Liu · Gang Li · Haiyan Song

Received: 1 October 2008 / Accepted: 12 November 2008 / Published online: 26 November 2008

Abstract Gold nanoparticles supported on TiO_2 were prepared using deposition–precipitation (DP) method and the catalysts were characterized by ICP, XRD, TEM, H_2-TPR, UV–Vis, NH_3-TPD and pyridine adsorbed FT-IR. The Au/TiO_2 was used to catalyze the aerobic oxidation of *n*-propyl alcohol dissolved in methanol and methyl propionate was synthesized. The results showed that 5% Au/TiO_2 calcined at 673 K exhibited excellent catalytic performance in direct synthesis of methyl propionate. The selectivity of methyl propionate could reach 99% and the maximum *n*-propyl alcohol conversion was 63%. Au/TiO_2 was stable and it could be reused for 6 cycles without significant deactivation when a base additive was added. The base dramatically improved the activity of gold catalysts and decelerated the deactivation of Au/TiO_2.

Keywords Gold catalyst · Oxidative esterification · Methyl propionate · Aerobic oxidation

1 Introduction

In recent years, heterogeneous gold catalysts have attracted extensive attentions and they have been applied to a variety of reactions, such as the oxidation of CO [1, 2], the oxidation of alcohol [3–5] and aldehyde [6, 7], water–gas shift reaction [8, 9], direct synthesis of hydrogen peroxide from H_2 and O_2 [10–13] and so on. Very recently, selective oxidation of 1, 4-butanediol [14] and catalytic transfer hydrogenation reaction [15] have been investigated. Some reactions will be industrialized. Meanwhile, the investigations of new reactions over gold catalysts are in progress. A great many potential applications of gold catalysts are probably to be carried out due to their high activity and less pollution to the environment.

Methyl esters have been used in organic synthesis as intermediate. The addition of methyl ester ethoxylates also gives detergent manufacturers another choice from the ethoxylate menu [16]. They are considered to be promising and prospective alternative diesel fuels to fossil diesel fuels and their roles as specific additives can be substantially more important [17, 18]. However, the conventional route of producing methyl esters in which a two-step synthetic procedure first involving the synthesis of carboxylic acids is required. What's more, the catalysts are mainly superacid, heteropoly acids and concentrated sulfuric acid which are of high toxicity and erosion. Although oxidative esterification of alcohols over Pd catalyst was already reported, the Pd catalyst has a problem of catalyst deactivation [19]. So a kind of stable and environmental friendly catalyst and a new reaction route are required for the synthesis of methyl esters.

According to Su et al. [20], facile oxidative transformation of alcohols, aldehydes, and acetals into esters has been carried out over Au/β-Ga_2O_3 with high activity and selectivity. In this paper, supported gold catalysts prepared by DP method are used in the oxidation of *n*-propyl alcohol dissolved in methanol to synthesize methyl propionate. This direct synthesis of methyl propionate was investigated and the reaction conditions were optimized. This new route is attractive due to the economic and environmental benefits of the oxidative esterification procedure. In addition, gold catalyst is easy to prepare and it has slight pollution to the environment.

G. Liu · G. Li (✉) · H. Song
State Key Laboratory of Fine Chemicals, Department of Catalytical Chemistry and Engineering, Dalian University of Technology, 116012 Dalian, China
e-mail: liganghg@dlut.edu.cn

2 Experimental

2.1 Catalyst Preparation

Au/TiO_2 catalysts were prepared by DP method using urea as the precipitator. Firstly, $HAuCl_4 \cdot 3H_2O$ (0.025 mol/L) as gold precursor was dissolved in 60 ml of deionized water. 1.0 g TiO_2 (commercial Degussa P25) together with 0.9 g urea were added. The mixture was stirred and heated to 353 K, then kept on stirring for 6 h, during which the pH value gradually increased from 3 to 8. The slurry was cooled to room temperature, then filtered and washed three times with deionized water, dried in air for 3 h at 373 K, then calcined in air for 4 h at 473–773 K. The catalysts with different supports were prepared using the same method as described above.

2.2 Catalyst Characterization

The inductively coupled plasma (ICP) was taken by American Plasma-Spec-II.Leeman to confirm the actual gold loaded on the support TiO_2. The XRD patterns were recorded on Rigaku D/Max 2400 diffractometer employing Cu Kα radiation. The FEI Tecnai G220 Stwin TEM was used to observe the morphology of the gold nanoparticles. The UV–Vis spectra were recorded using Jasco UV-550 spectrophotometer. Hydrogen temperature-programmed reduction (H_2-TPR) measurement was carried out in homemade equipment with a thermal conductivity detector (TCD GC 7890T). A total of 50 mg catalyst was filled in a quartz reactor. The catalyst was pretreated in N_2 flow (40 ml/min) at 373 K for 1 h before TPR analysis in order to eliminate water. The TPR results were obtained by heating the samples under 10% H_2/N_2 with the flow rate of 40 ml/min. The temperature was linearly raised from 303 to 1073 K at the rate of 10 K/min. Temperature-programmed desorption of ammonia (NH_3-TPD) was carried out in homemade equipment with a thermal conductivity detector (TCD GC 7890T). A 50 mg sample was dried in N_2 flow (40 ml/min) at 373 K for 1 h, and then cooled to 303 K to absorb NH_3. Desorption of NH_3 was performed in N_2 flow (40 ml/min) by increasing the temperature to 773 K at the rate of 10 K/min. The pyridine absorbed FT-IR spectra were recorded using Bruker EQUINOX55 infrared spectrometer.

2.3 Reaction

The following procedure was used in the direct synthesis of methyl propionate. Firstly, methanol, *n*-propyl alcohol and catalyst were charged in an autoclave with a polytetrafluoroethylene-liner. A desired amount of additive ($NaHCO_3$, Na_2CO_3, K_2CO_3, $NaOCH_3$ or NaOH) was added. The autoclave was charged with 5–20 atm oxygen, then stirred and heated to the target temperature. As the autoclave cooled to room temperature, the product was analyzed by Agilent GC-6890N (HP-5 capillary pole, Flame Ionization Detector). For the recycling test, the Au/TiO_2 catalyst was recovered, dried in air at 373 K for 3 h and then used in the next run with fresh reagent.

3 Results and Discussion

3.1 Catalyst Characterization

3.1.1 ICP

The ICP result of Au/TiO_2 prepared by DP-urea suggests that the actual gold loading (4.94%) is in well agreement with the expected theoretical value (5%). Therefore, Au/TiO_2 catalyst prepared by DP-urea exhibits very high use ratio of gold and there is almost no loss of gold during the preparation.

3.1.2 XRD

Figure 1 shows the XRD patterns of Au/TiO_2 with different gold loadings. Compared with pure TiO_2, 2.5% Au/TiO_2 does not exhibit obvious gold peaks in XRD pattern. There are only slight gold peaks when the gold loading increases to 5%. This may be due to the fact that the corresponding gold particles are too small to be detected [21]. According to Huang et al. [14], gold particles are closely packed and could congregate easily when the gold loading up to 8%, leading to a higher average of

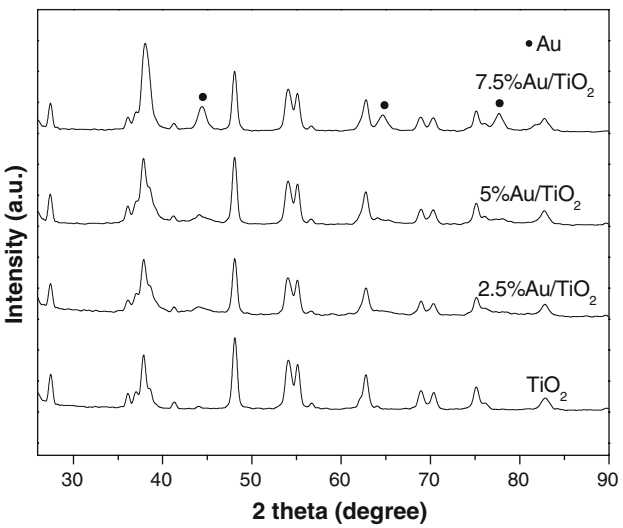

Fig. 1 XRD patterns of Au/TiO_2 with different gold loadings calcined at 673 K

gold particle size. In our work, intense gold peaks of (200), (220) and (311) at 44.4°, 64.4° and 77.4°, respectively, can be seen as the gold loading increasing to 7.5%. XRD patterns of samples calcined at different temperatures are shown in Fig. 2. There is no significant difference of gold peaks as the catalyst calcined at a lower temperature of 473 and 573 K. Further increase of calcination temperature results in the agglomeration of gold particles, with the gradual intense appearance of gold diffraction peaks. In a word, high calcination temperature and high gold loading lead to the agglomeration of gold particles.

3.1.3 TEM

TEM image in Fig. 3 shows the gold particle size ranges from 4 to 7 nm with a uniform distribution. Hundred such particles were counted in TEM image in order to confirm the gold distribution (histogram in Fig. 4). The nature of active sites in supported gold catalysts has been discussed previously [22, 23]. Accordingly, the metallic gold particles on the support TiO_2 which can be seen in the TEM image may contribute to the active sites of Au/TiO_2.

3.1.4 UV–Vis

Figure 5 shows UV–Vis spectra of Au/TiO_2 with different gold loadings. The absorbance from 200 to 350 nm is assigned to the TiO_2 support and the absorption around 550 nm owns to the metallic gold nanoparticles. For Au/TiO_2 catalyst, the intensity of absorbance band is related to the size of gold particles and the content of gold in Au/TiO_2 [24]. Accordingly, higher gold loading contributes to a greater average of gold particle size, which is well agreed with the XRD result (Fig. 1). Figure 6 shows

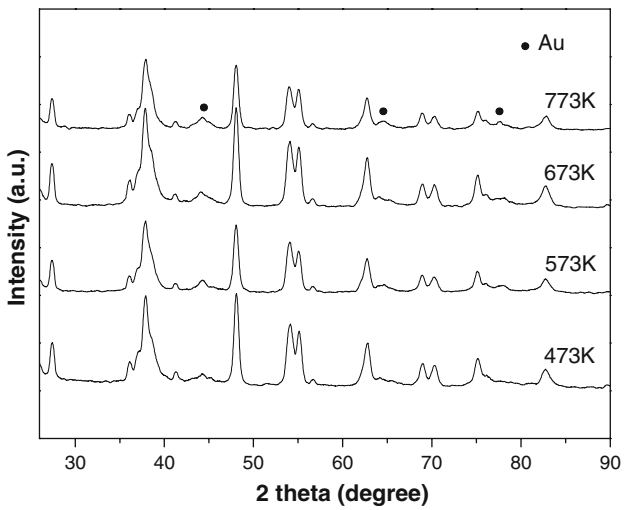

Fig. 2 XRD patterns of 5% Au/TiO_2 calcined at 473, 573, 673, and 773 K

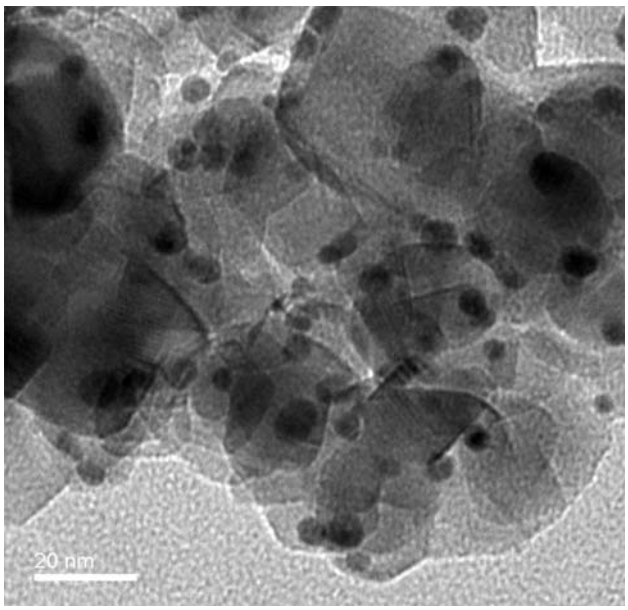

Fig. 3 TEM image of 5% Au/TiO_2 calcined at 673 K

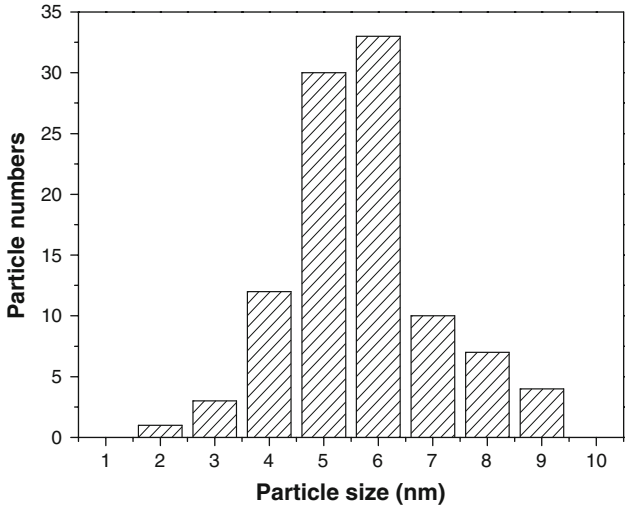

Fig. 4 Gold particle size distribution of 5% Au/TiO_2 calcined at 673 K

UV–Vis spectra of 5% Au/TiO_2 calcined at different temperatures. The metallic gold is only partially formed after being calcined at 373 K. A strong peak near 550 nm is observed as the sample calcined at 473, 573, 673 and 773 K which suggests that gold has been reduced under these temperatures. The gold peak is a little higher after being calcined at a higher temperature owning to larger gold particles.

3.1.5 H_2-TPR

H_2-TPR is used to study the reducibility of gold on TiO_2. As shown in Fig. 7, a single reduction peak can be

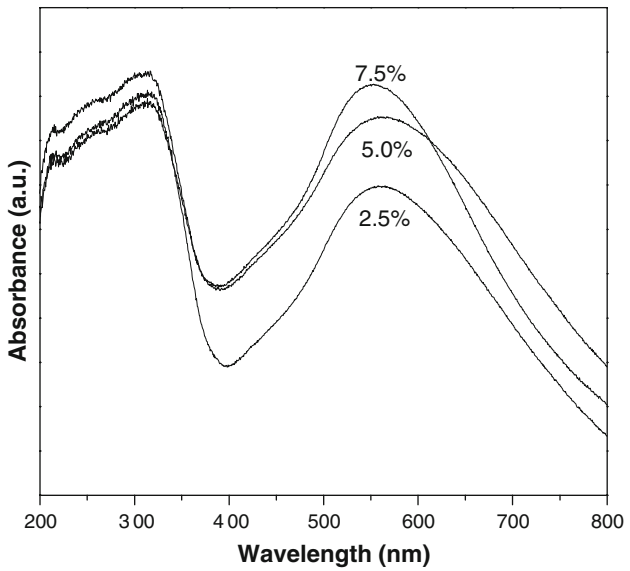

Fig. 5 UV–Vis spectra of Au/TiO_2 with different gold loadings calcined at 673 K

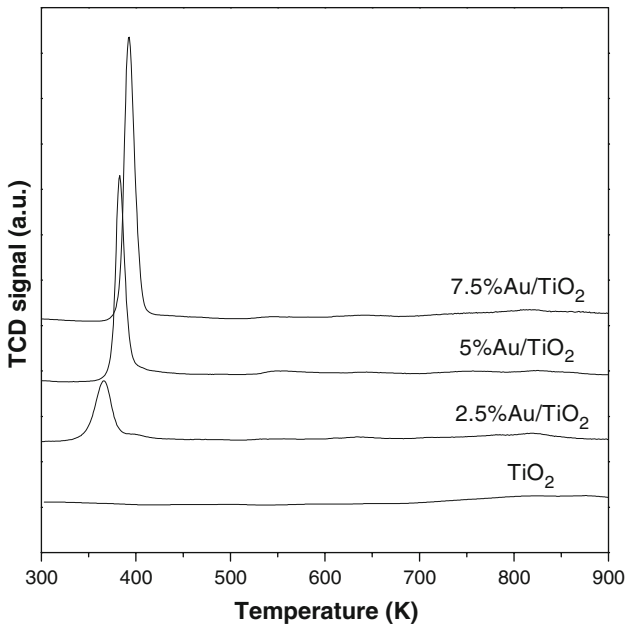

Fig. 7 H_2-TPR spectra of Au/TiO_2 with different gold loadings

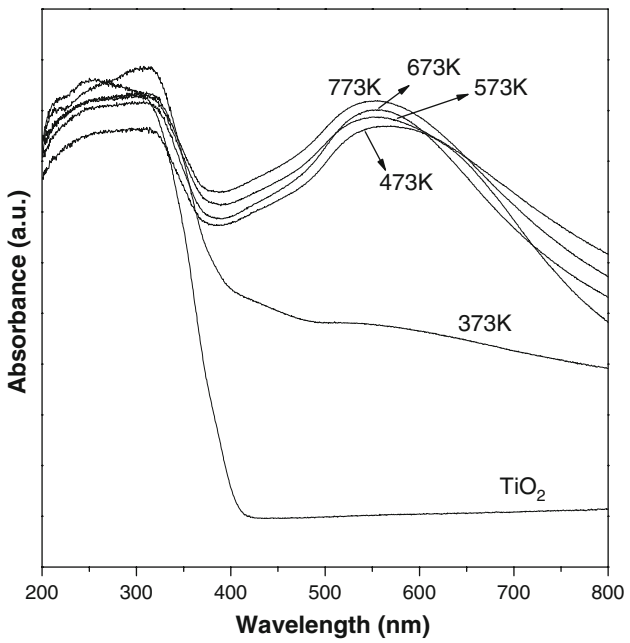

Fig. 6 UV–Vis spectra of 5% Au/TiO_2 calcined at 373, 473, 573, 673, and 773 K

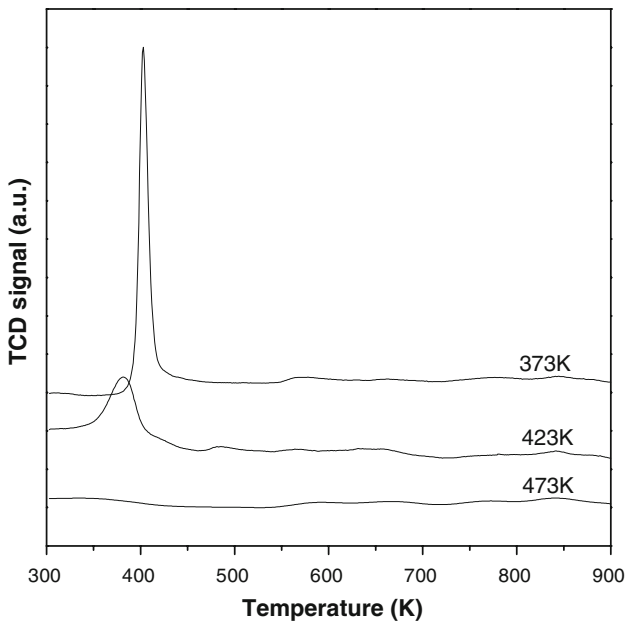

Fig. 8 H_2-TPR spectra of 5% Au/TiO_2 treated at 373, 423, and 473 K

observed at 370–400 K. With the gold loading increasing from 2.5 to 7.5%, the peaks shift to higher temperature because the gold are more difficult to be reduced with a higher gold loading. TPR spectra of 5% Au/TiO_2 treated at different temperatures in N_2 flowing are shown in Fig. 8. Gold reduction peak is much lower as treated at 423 K than that of 373 K and there is an obvious peak shift to lower temperature. The reduction peak of 5% Au/TiO_2 treated at 423 K is similar to the TPR spectrum of 2.5% Au/TiO_2 (shown in Fig. 7) both in the intensity and position. This can be explained by that gold is partly reduced after being treated in N_2 flowing at 423 K, and the unreduced gold on the TiO_2 support is much easier to be reduced in H_2 flowing. As being treated at 473 K, the reduction peak disappears because the gold has been completely reduced at this temperature.

3.2 Catalytic Performance in Esterification

In this section, different supported gold catalysts prepared by DP method are used in the synthesis of methyl propionate. All the gold catalysts exhibit excellent selectivity of methyl propionate, while the conversion of *n*-propyl alcohol is disparate (Table 1). Au/TiO_2 is the most active catalyst among them. The effect of support was reported previously. According to Abad et al. [25], the support not only has the role of stabilizing the nanoparticles, but also has a synergic effect with gold. Haruta [23] indicated that the catalytic performances of gold markedly depend on the supports and Mavrikakis et al. [26] reported that the catalytic activity of highly dispersed Au particles may be partly due to high step densities on the small particles and/or strain effects due to the mismatch at the Au-support interface. Therefore, the effect of Au-support strain is different and gold particles loading on different supports can display disparate size, which cause the difference of catalytic activity.

According to Li et al. [27] and Zhu et al. [28], the presence of base can dramatically boost the catalytic activity of gold catalysts. Meanwhile, methyl ester product does not consume base, thus a small amount of base is capable to promote the reaction. In the presence of base, the hydrogen is readily abstracted from the primary hydroxyl and this overcomes the rate limiting step for the oxidation process [29–31]. In our work, with the additive of base, there are significant increase in *n*-propyl alcohol conversion and slight increase of methyl propionate selectivity. Similar results can be obtained by using different bases. The results of blank experiments without gold catalyst but only in the presence of a base indicate that the base has no catalytic activity (Table 1). We also did other blank experiments in the presence of a base together with support TiO_2, but no *n*-propyl alcohol oxidation happened. Therefore, gold catalyst is indispensable in the reaction.

Table 2 shows the effect of catalyst weight and gold loading of Au/TiO_2 on the esterification. An increase of *n*-propyl alcohol conversion is obtained with the increase of catalyst weight, but TOF decreases at the same time. Gold loading has a significant effect on the activity of Au/TiO_2 and 5% Au/TiO_2 is optimal. With equal weight of catalyst, 7.5% Au/TiO_2 shows a lower activity than that of 5% Au/TiO_2. This should be attributed to the increase of gold particle size with increasing gold loading. With the higher gold loading and greater amount of catalyst, the turnover number corresponding to gold active sites is much lower. While the catalyst weight and gold loading seem to have no effect on the methyl propionate selectivity.

Table 3 shows the effect of calcination temperature of Au/TiO_2 on *n*-propyl alcohol conversion. The Au/TiO_2 catalyst calcined at 373 K exhibits no catalytic activity, owing to that gold is only partially reduced under this temperature. Catalyst calcined at 673 K exhibits the highest activity. Further increase of calcination temperature results in the decrease of catalytic activity, which can be attributed to the sintering of gold particles (XRD patterns in Fig. 2 and UV–Vis spectra in Fig. 6).

In this reaction system, methanol plays both as solvent and reactant. As shown in Fig. 9, with high molar ratio of *n*-propyl alcohol/methanol (1:2), the conversion of *n*-propyl alcohol and the selectivity of methyl propionate are low. With decreasing the molar ratio, higher *n*-propyl

Table 1 Results of direct synthesis of methyl propionate over various gold supported catalysts and additives

Catalysts	Additives	*n*-Propyl alcohol conversion (%)	Methyl propionate selectivity (%)	Methyl propionate yield (%)	TOFs (h^{-1})	TOFs (mol $g^{-1}_{(Au)}$ h^{-1})
None	$NaHCO_3$	0	–	0	0	0
None	NaOH	0	–	0	0	0
TiO_2^a	$NaHCO_3$	0	–	0	0	0
TiO_2^b	NaOH	0	–	0	0	0
Au/TiO_2	None	17.8	93.5	15.7	81	0.41
Au/TiO_2	Na_2CO_3	37.9	96.1	35.0	183	0.93
Au/TiO_2	$NaHCO_3$	36.8	96.2	34.1	172	0.87
Au/TiO_2	K_2CO_3	35.3	96.2	32.8	157	0.81
Au/TiO_2	$NaOCH_3$	37.9	96.0	35.0	183	0.93
Au/TiO_2	NaOH	36.3	96.0	33.5	162	0.82
Au/SiO_2	None	12.8	92.6	11.0	62	0.32
Au/SiO_2	$NaHCO_3$	25.8	95.0	23.4	126	0.64
Au/Al_2O_3	$NaHCO_3$	33.0	95.7	30.2	159	0.81
Au/Fe_2O_3	$NaHCO_3$	21.0	95.5	19.1	101	0.51
Au/MgO	$NaHCO_3$	7.4	93.0	6.5	36	0.18

Reaction conditions: 30 ml *n*-propyl alcohol/methanol with molar ratio 1:8, 0.2 g catalyst calcined at 673 K with gold loading 5%, molar ratio of additive/*n*-propyl alcohol 0.01, charged with 15 atm oxygen, reaction temperature 393 K, reaction time 3 h

[a,b] TiO_2 was calcined at 673 K

Table 2 Effect of catalyst weight and gold loading of Au/TiO_2 calcined at 673 K

Catalysts amount (g)	Gold loading (%)	*n*-Propyl alcohol conversion (%)	Methyl propionate selectivity (%)	Methyl propionate yield (%)	TOFs (h^{-1})	TOFs (mol $g^{-1}_{(Au)}$ h^{-1})
0.1	2.5	18.9	95.6	17.3	387	1.97
0.2	2.5	25.4	95.8	23.3	260	1.32
0.3	2.5	30.9	96.0	28.5	207	1.05
0.1	5.0	30.3	95.7	27.8	282	1.43
0.2	5.0	36.8	96.2	34.1	172	0.87
0.3	5.0	40.0	96.2	37.1	132	0.67
0.1	7.5	22.6	96.1	20.9	161	0.82
0.2	7.5	34.9	95.8	32.1	116	0.59
0.3	7.5	40.0	96.2	37.0	94	0.48

Reaction conditions: Au/TiO_2 with different weights and gold loadings, 30 ml *n*-propyl alcohol/methanol with molar ratio 1:8, $NaHCO_3$/*n*-propyl alcohol molar ratio 0.01, charged with 15 atm oxygen, reaction temperature 393 K, reaction time 3 h

Table 3 Effect of calcination temperature of Au/TiO_2 on *n*-propyl alcohol conversion

Calcination temperature (K)	*n*-Propyl alcohol conversion (%)	Methyl propionate selectivity (%)	Methyl propionate yield (%)	TOFs (h^{-1})	TOFs (mol $g^{-1}_{(Au)}$ h^{-1})
373	0	–	0	0	0
473	31.8	96.4	29.6	112	0.57
573	33.1	96.2	30.7	114	0.58
673	34.9	95.8	32.1	116	0.59
773	26.7	95.8	24.5	94	0.48

Reaction conditions: 0.2 g 7.5% Au/TiO_2 calcined at different temperatures, other conditions are same as Table 2

alcohol conversion and methyl propionate selectivity are obtained due to the great amount of solvent methanol. Figure 10 shows the effect of oxygen pressure on the oxidation of *n*-propyl alcohol. Increasing the pressure of oxygen can dramatically improve the conversion of *n*-propyl alcohol, which indicates the presence of great amount of oxygen can intensify the oxidation of *n*-propyl alcohol. But the pressure of oxygen has no obvious effect on the selectivity of methyl propionate.

Increase of the reaction temperature improves the *n*-propyl alcohol conversion, while further increase of reaction temperature results in a decrease of *n*-propyl alcohol conversion after 393 K (Table 4). We proposed that at high temperature methyl propionate is unstable and

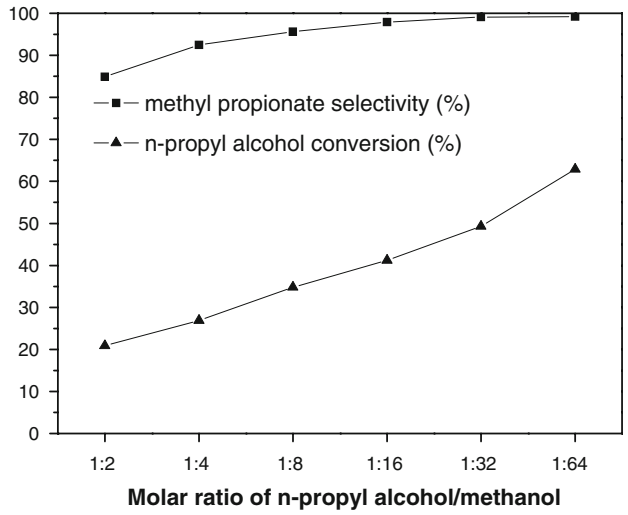

Fig. 9 Effect of *n*-propyl alcohol/methanol molar ratio on the oxidation of *n*-propyl alcohol. Reaction conditions: 0.2 g 5% Au/TiO_2, *n*-propyl alcohol/methanol with different molar ratios, other conditions are same as Table 2

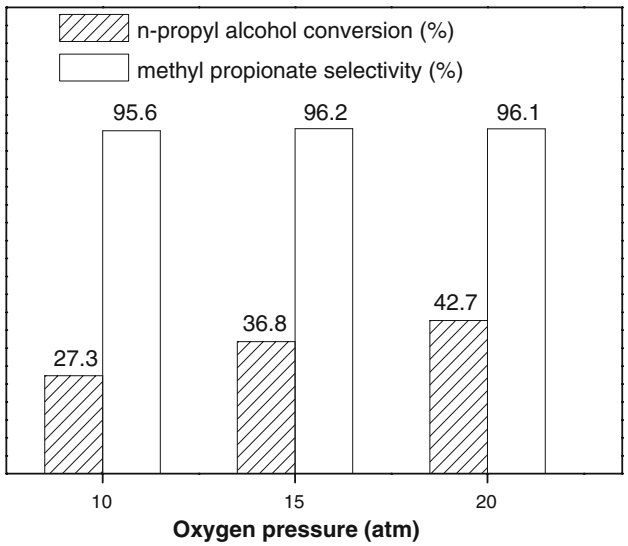

Fig. 10 Effect of oxygen pressure on the oxidation of *n*-propyl alcohol. Reaction conditions: 0.2 g 5% Au/TiO_2, charged with different pressure of oxygen, other conditions are same as Table 2

Table 4 Effect of reaction temperature on the oxidation of *n*-propyl alcohol

Reaction temperature (K)	*n*-Propyl alcohol conversion (%)	Methyl propionate selectivity (%)	Methyl propionate yield (%)	TOFs (h^{-1})	TOFs (mol $g^{-1}_{(Au)}$ h^{-1})
373	23.3	95.8	21.4	116	0.59
393	36.8	96.2	34.1	183	0.93
413	33.3	95.8	30.6	168	0.85

Reaction conditions: 0.2 g 5% Au/TiO_2, different reaction temperatures, other conditions are same as Table 2

easy to decompose due to the reversibility of esterification. We also studied the effect of stirring rate on *n*-propyl alcohol conversion. The result shows that low rate of stirring can not provide sufficient mixing intensity of the reagent and catalyst. At least 500 rpm of stirring rate is required to overcome the diffusion barrier.

Effect of reaction time on *n*-propyl alcohol conversion and methyl propionate selectivity with the additive of $NaOCH_3$ is shown in Fig. 11. The reaction rate is rapid during the first 0.5 h, with the *n*-propyl alcohol conversion of 23% and a very high $TOF_{t\ =\ 0.5\ h}$ of 609. The methyl propionate selectivity maintains at about 96% during the reaction process, with a small amount of by-product propyl propionate (about 4%). As reaction proceeds, reaction rate becomes slow. After 3 h, the *n*-propyl alcohol conversion achieves a maximum of 38%. Further increase of reaction time does not promote the conversion of *n*-propyl alcohol which means the equilibrium is reached.

3.3 Recycling Test

The durability of Au/TiO_2 in this reaction is studied. In the presence of base, during the usage of first 6 cycles, there is no obvious decrease of catalytic activity (Fig. 12). Only a slight decrease occurs in further usage. While in the absence of base, the catalyst suffers some deactivation and even has no activity in the seventh cycle (Fig. 13). Interestingly, the activity of Au/TiO_2 recovers after being washed with NaOH 5 M. In order to determine the causes of deactivation, the deactivated catalyst is characterized by XRD, TEM, UV–Vis, ICP, NH_3-TPD and pyridine adsorbed FT-IR spectroscopy. The XRD, TEM and UV–Vis results of deactivated catalyst show no difference with fresh catalyst, which means the size and distribution of gold particles do not change after spent for 9 cycles. The ICP result shows that the gold loading decreases from 4.94 to 4.47%. However, a slight decrease of gold loading can not result in the extent of deactivation (with the conversion of *n*-propyl alcohol decreases from 36 to 27%) because gold loading of 2.5% can achieve the *n*-propyl alcohol conversion 25% (Table 3). In addition, the base can not only boost the conversion of *n*-propyl alcohol and the selectivity of methyl propionate, but also decelerate the deactivation rate of Au/TiO_2.

NH_3-TPD results of the deactivated catalyst are given in Fig. 14. One NH_3 desorption peak can be observed at

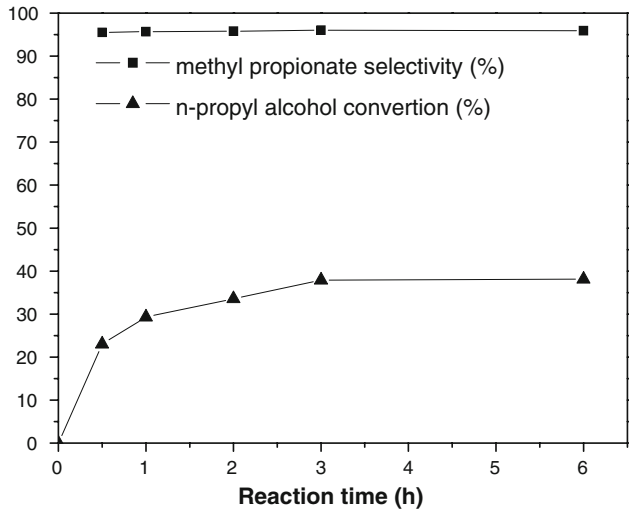

Fig. 11 Effect of reaction time on *n*-propyl alcohol conversion and methyl propionate selectivity. Reaction conditions: 0.2 g 5% Au/TiO_2, $NaOCH_3$/*n*-propyl alcohol molar ratio 0.01, react for different period of times, other conditions are same as Table 2

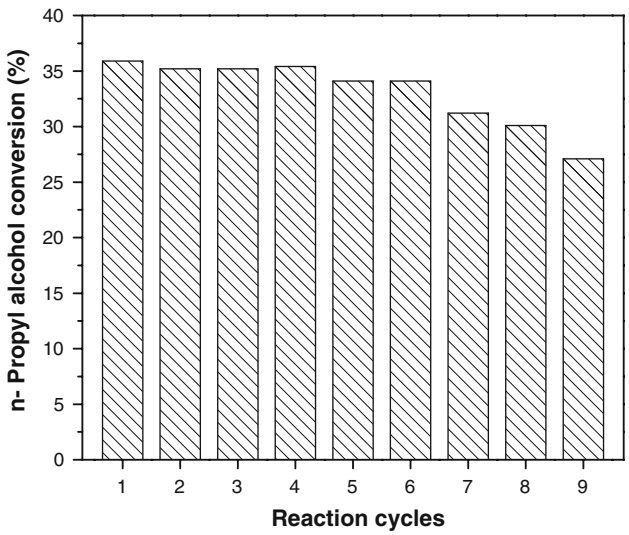

Fig. 12 Long-term stability of Au/TiO_2 in oxidative esterification in the presence of base. Reaction conditions: 0.2 g 5% Au/TiO_2, other conditions are same as Table 2

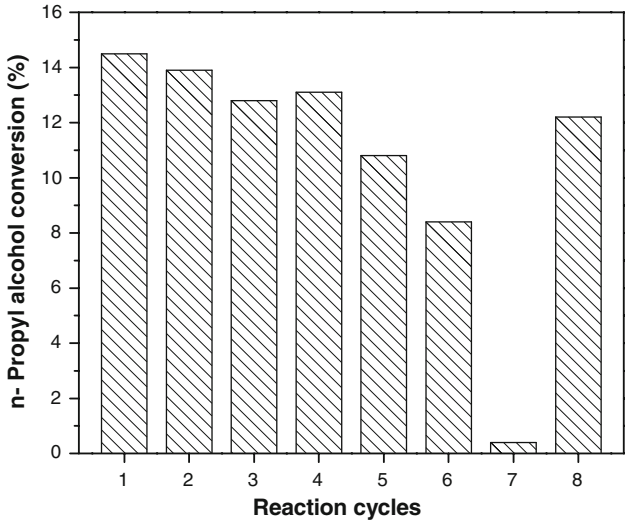

Fig. 13 Long-term stability of Au/TiO_2 in oxidative esterification in the absence of base. Reaction conditions: 0.2 g 5% Au/TiO_2, without the addition of base, other conditions are same as Table 2. The deactivated catalyst in the seventh cycle was submerged in NaOH 5 M and stirred for 0.5 h, washed exhaustively with deionized water, dried in air at 373 K for 3 h, and then used in the eighth cycle

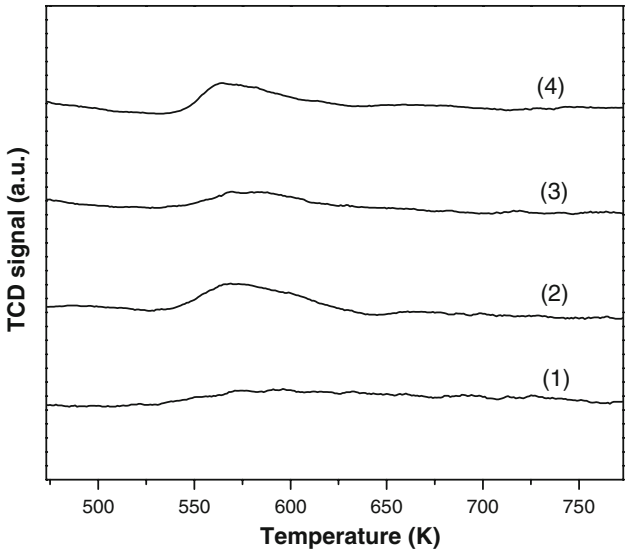

Fig. 14 NH_3-TPD of 5% Au/TiO_2: (1) fresh; (2) spent for 7 cycles; (3) spent for 7 cycles and washed by NaOH 5 M; (4) spent for 7 cycles and recalcined in air at 673 K for 4 h

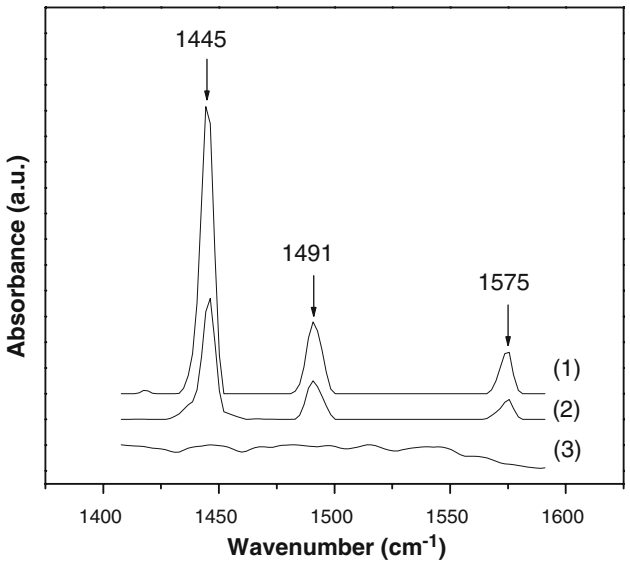

Fig. 15 FT-IR spectra of pyridine adsorbed on Au/TiO_2 after evacuation at: (1) 423 K; (2) 573 K; (3) 723 K

around 570 K for deactivated catalyst which ascribes to the existence of acidic sites on the surface of the sample. The Au/TiO_2 catalyst previously calcined at 673 K, deactivated after being used for 7 cycles, was recalcined in air at 673 K for 4 h, but the activity of Au/TiO_2 can not be recovered. The desorption peak in NH_3-TPD of this sample has no difference with that of the deactivated catalyst, which means the acidic sites has no transformation. The result of pyridine absorbed FT-IR spectroscopy was shown in Fig. 15. The IR absorption bands at 1445, 1491 and 1575 cm^{-1} are ascribed to Lewis sites [32]. In addition, only a slight desorption peak for the deactivated catalyst could be seen after being washed with NaOH 5 M (Fig. 14) which indicates that most of the Lewis sites have been eliminated. Konova et al. [33] proposed that the formation of oxygen vacancies (Lewis sites) on Au/TiO_2 surface leads to the decreasing of catalytic activity. The pyridine absorbed FT-IR results in our work show that Lewis sites are formed on the deactivated catalyst. So we suppose that the formation of oxygen vacancies on Au/TiO_2 causes the catalyst deactivation and NaOH washing can fill up the oxygen vacancies and recover the catalyst activity. However, the reason of catalyst deactivation is still unclear and more experiments are necessary to elucidate the nature of catalyst deactivation. Further study of catalyst deactivation in esterification is in progress.

3.4 Mechanism of Esterification

The mechanism for the synthesis of methyl propionate over Au/TiO_2 is proposed in Scheme 1. The catalytic esterification will go through three steps. The first step will be the oxidation of *n*-propyl alcohol, in which the abstraction of hydrogen from *n*-propyl alcohol and the formation of propyl aldehyde take place. The second step is the formation of hemiacetals and acetals. Methyl propionate and propyl propionate are formed by the oxidation of hemiacetals in the last step. The first step could be the rate-determining step since no propyl aldehyde, hemiacetals or acetals is detected during the reaction, so propyl aldehyde, hemiacetals or acetals may rapidly react further. The base additive which can promote the abstraction of hydrogen in

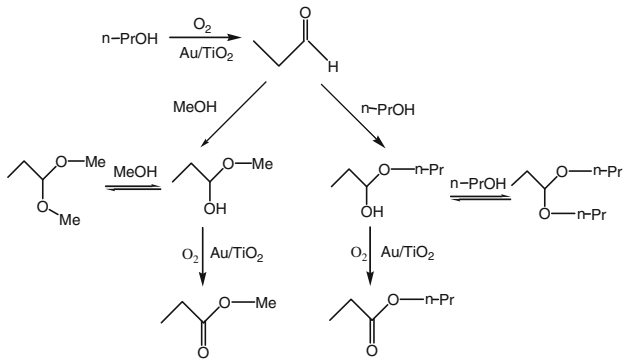

Scheme 1 Reaction scheme for esterification of *n*-propyl alcohol and methanol over Au/TiO_2

the first step can increase the conversion of *n*-propyl alcohol. According to Su et al. [20], hemiacetal formation from aldehydes and alcohols is a facile reaction due to the good electrophilic properties of aldehydes and nucleophilic properties of alcohols, and may not require a catalyst. Therefore, propanoic acid can not be formed because propyl aldehyde can rapidly react with methanol and *n*-propyl alcohol to form methyl propionate and propyl propionate. Although this reaction actually goes through three steps, the absence of propyl aldehyde, hemiacetals or acetals in any moment of reaction makes it seem that *n*-propyl alcohol and methanol directly convert to methyl propionate, so we define it as direct synthesis of methyl propionate.

4 Conclusions

In this work, direct synthesis of methyl propionate with *n*-propyl alcohol dissolved in methanol was investigated. A series of gold supported catalysts prepared by DP method exhibited high activity and selectivity. Five percentage of Au/TiO_2 calcined at 673 K exhibited the highest activity. The reaction temperature and oxygen pressure had great effects on the reaction. The Au/TiO_2 catalyst showed attractive stability and it could be reused for 6 cycles without significant deactivation when a base additive was added. The presence of base dramatically improved the activity of gold catalysts and decelerated the deactivation rate of Au/TiO_2. In this reaction system, target product methyl propionate achieved high selectivity and the minor propyl propionate was the only by-product.

Acknowledgments The Project is sponsored by the Foundation for the Author of National Excellent Doctoral Dissertation of PR China (No. 200346), Program for New Century Excellent Talents in University (NCET-04-0270), National Natural Science Foundation of China (No. 20406005) and the Scientific Research Foundation for the Returned Overseas Chinese Scholars, State Education Ministry.

References

1. Zanella R, Giorgio S, Shin CH, Henry CR, Louis C (2004) J Catal 222:357–367
2. Qian K, Huang WX, Fang J, Lv SS, He B, Jiang ZQ, Wei SQ (2008) J Catal 255:269–278
3. Su FZ, Chen M, Wang LC, Huang XS, Liu YM, Cao Y, He HY, Fan KN (2008) Catal Commun 9:1027–1032
4. Zheng NF, Stucky GD, (2007) Chem Commun 3862–3864
5. Yang XM, Wang XN, Liang CH, Su WG, Wang C, Feng ZC, Li C, Qiu JS (2008) Catal Commun 9:2278–2281
6. Marsden C, Taarning E, Hansen D, Johansen L, Klitgaard SK, Egeblad K, Christensen CH (2008) Green Chem 10:168–170
7. Biella S, Prati L, Rossi M, Mol J (2003) Catal A Chem 197:207–212
8. Idakiev V, Yuan ZY, Tabakova T, Su BL (2005) Appl Catal A Gen 281:149–155
9. Li JW, Zhan YY, Zhang FL, Lin XY, Zheng Q (2008) Chin J Catal 29(4):346–350
10. Li G, Edwards J, Carley AF, Hutchings GJ (2007) Catal Commun 8:247–250
11. Li G, Edwards J, Carley AF, Hutchings GJ (2006) Catal Today 114:369–371
12. Li G, Edwards J, Carley AF, Hutchings GJ (2007) Catal Today 122:361–364
13. Ma SQ, Li G, Wang XS (2006) Chem Lett 35(4):428–429
14. Huang J, Dai WL, Li HX, Fan KN (2007) J Catal 252:69–76
15. Su FZ, He L, Ni J, Cao Y, He HY, Fan KN (2008) Chem Commun 3531–3533
16. Cox MF, Weerasooriya U (1997) JAOCS Vol 74(7):847–859
17. Kocsisová T, Cvengroš J, Lutišan J (2005) Eur J Lipid Sci Technol 107:87–92
18. Cvengroš J, Paligová J, Cvengrošová Z (2006) Eur J Lipid Sci Technol 108:629–635
19. Hayashi T, Inagaki T, Itayama N, Baba H (2006) Catal Today 117:210–213
20. Su FZ, Ni J, Sun H, Cao Y, He HY, Fan KN (2008) Chem Eur J 14:7131–7135
21. Chang FW, Yu HY, Roselin LS, Yang HC (2005) Appl Catal A Gen 290:138–147
22. Valden M, Paka S, Lai X, Goodman DW (1998) Catal Lett 56:7–10
23. Haruta M (1997) Catal Today 36:153–166
24. Tian BZ, Zhang JL, Tong TZ, Chen F (2008) Appl Catal B 79:394–401
25. Abad A, Corma A, Garcia H (2008) Chem Eur J 14:212–222
26. Mavrikakis M, Stoltze P, Nørskov JK (2000) Catal Lett 64:101–106
27. Li HR, Guan BT, Wang WJ, Dong X, Zhao F, Wan XB, Yang LP, Shi ZJ (2007) Tetrahedron Lett 63:8430–8434
28. Zhu JJ, Figueiredo JL, Faria JL (2008) Catal Commun 9:2395–2397
29. Esben T, Anders TM, Jorge MM, Kresten E, Claus HC (2008) Green Chem 10:408–414
30. Carrettin S, McMorn P, Johnston P, Griffin K, Hutchings GJ (2002) Chem Commun 696–697
31. Carrettin S, McMorn P, Johnston P, Griffin K, Kielyc CJ, Hutchings GJ (2003) Phys Chem Chem Phys 5:1329–1336
32. Centi G, Golinelli G, Busca G (1990) J Phys Chem 94:6813–6819
33. Konova P, Naydenov A, Venkov C, Mehandjiev D, Andreeva D, Tabakova T, Mol J (2004) Catal A Chem 213:235–240